Accuracy of automatic abnormal potential annotation for substrate identification in scar-related ventricular tachycardia

Short Title: Nakatani, et al. automatic identification of VT substrates

Yosuke Nakatani, MD[1]; Philippe Maury, MD[2]; Anne Rollin, MD[2]; F. Daniel Ramirez, MD[1]; Cyril Goujeau, MD[1]; Takashi Nakashima, MD[1]; Clémentine André, MD[1]; Aline Carapezzi, BE[3]; Philipp Krisai, MD[1]; Takamitsu Takagi, MD[1]; Tsukasa Kamakura, MD, PhD[1]; Konstantinos Vlachos, MD[1]; Ghassen Cheniti, MD[1]; Romain Tixier, MD[1]; Quentin Voglimacci-Stefanopoli, MD[2] , Nicolas Welte, MD[1]; Remi Chauvel, MD[1]; Josselin Duchateau, MD[1]; Thomas Pambrun, MD[1]; Nicolas Derval, MD[1]; Mélèze Hocini, MD[1]; Michel Haïssaguerre, MD[1]; Pierre Jaïs, MD[1]; Frédéric Sacher, MD[1]

[1] Department of Cardiac Pacing and Electrophysiology, IHU Liryc, Electrophysiology and Heart Modeling Institute, Univ. Bordeaux, Bordeaux University Hospital (CHU), Pessac- Bordeaux, France
[2] Unité Inserm U 1048, University Hospital Rangueil, Toulouse, France
[3] Boston Scientific, France

Address for correspondence: Dr. Yosuke Nakatani, Department of Cardiac Pacing and Electrophysiology, IHU Liryc, Electrophysiology and Heart Modeling Institute, Univ. Bordeaux, Bordeaux University Hospital (CHU), Avenue de Magellan, 33604 Pessac-Bordeaux, France. Telephone: +33-5-57656542; Fax: +33-5-57656509; E-mail: yosuke3gbst@gmail.com

ABSTRACT

Introduction: Ultra-high-density mapping for ventricular tachycardia (VT) is increasingly used. However, manual annotation of local abnormal ventricular activities (LAVAs) is challenging in this setting. Therefore, we assessed the accuracy of the automatic annotation of LAVAs with the Lumipoint algorithm of the Rhythmia system (Boston Scientific).

Methods and Results: One hundred consecutive patients undergoing catheter ablation of scar-related VT were studied. Areas with LAVAs and ablation sites were manually annotated during the procedure and compared with automatically annotated areas using the Lumipoint features for detecting late potentials (LP), fragmented potentials (FP), and double potentials (DP). The accuracy of each automatic annotation feature was assessed by re-evaluating local potentials within automatically annotated areas. Automatically annotated areas matched with manually annotated areas in 64 cases (64%), identified an area with LAVAs missed during manual annotation in 15 cases (15%), and did not highlight areas identified with manual annotation in 18 cases (18%). Automatic FP annotation accurately detected LAVAs regardless of the cardiac rhythm or scar location; automatic LP annotation accurately detected LAVAs in sinus rhythm, but was affected by the scar location during ventricular pacing; automatic DP annotation was not affected by the mapping rhythm, but its accuracy was suboptimal when the scar was located on the right ventricle or epicardium.

Conclusion: The Lumipoint algorithm was as/more accurate than manual annotation in 79% of patients. FP annotation detected LAVAs most accurately regardless of mapping rhythm and scar location. The accuracy of LP and DP annotations varied depending on mapping rhythm or scar location.

Keywords: ventricular tachycardia; catheter ablation; local abnormal ventricular activities; late potential; fragmented potential; double potential; high-resolution mapping.

INTRODUCTION

The assessment of tachycardia circuit is a critical part of the ablation procedure for ventricular tachycardia (VT); however, VTs are often unmappable in clinical practice due to non-inducibility, multiple inducible VTs, and hemodynamic instability.[1,2] Moreover, even if VT is terminated by ablating an identified isthmus, other VT may still occur due to remaining substrates. Therefore, the elimination of potential VT substrates as identified by abnormal potentials, such as local abnormal ventricular activities (LAVAs) recorded during sinus rhythm or pacing, has become a widely used approach to VT ablation.[3-7]

Ultra-high-resolution mapping systems can help identify VT circuits;[8,9] however, high-density point collection renders manual annotation of LAVAs challenging. Moreover, the detection of LAVAs is suboptimal with conventional automatic annotation systems, which is based on a single activation time annotation to an electrogram peak in each point. A novel "Lumipoint" algorithm (Boston Scientific, Marlborough, MA) analyzes the complete electrogram tracing to determine activity at each location.[10-15] Since the activated surface in a given window of interest is highlighted with this algorithm, late potentials (LPs) can be detected by adjusting this window to cover the post-QRS phase.[10,11] Moreover, this algorithm can highlight areas with fragmented potentials (FPs) and double potentials (DPs). Therefore, LAVAs can be automatically detected by this algorithm. The present study sought to assess the accuracy of the Lumipoint algorithm to identify LAVAs in patients with scar-related VT.

METHODS

Study population

We retrospectively studied 100 consecutive patients with scar-related VT who underwent catheter ablation using a ultra-high-density mapping system (Rhythmia, Boston Scientific) at two tertiary centers (Bordeaux University Hospital, Bordeaux, France, and University Hospital Rangueil, Toulouse, France) between April 2015 to October 2019. According to the institutional guidelines, all patients gave written informed consent, with ethical approval.

Electrophysiological study and catheter ablation

A quadripolar catheter was placed at the right ventricular apex and a decapolar catheter was placed in the coronary sinus. Access to the left ventricular (LV) cavity was gained through an anterograde transseptal approach or retrograde transaortic approach, depending on clinical factors. If the clinical VT or pre-procedural imaging suggested an epicardial circuit, epicardial access was obtained. A steerable sheath (Agilis, St. Jude Medical Inc., St. Paul, MN) was used for mapping via transseptal or epicardial approaches.

Sequential contact mapping was performed using the Rhythmia system with a multipolar basket catheter (Orion, Boston Scientific). The following beat acceptance criteria were used: (1) electrocardiographic QRS morphology match; (2) temporal stability of electrograms; (3) respiratory gating; and (4) a maximal distance between the electrode and the anatomical shell of 2 mm. Bipolar electrograms were filtered at 30 and 300 Hz, and unipolar electrograms at 1 and 300 Hz without a notch filter. Substrate mapping was performed either in sinus rhythm or with pacing from the right ventricular (RV) apex (RV pacing) or lateral branch of the coronary sinus (LV pacing) at a cycle length of 600 ms. Areas with LAVAs were manually tagged during map acquisition. LAVAs were defined as sharp high-frequency ventricular potentials that are distinct from the far-field ventricular electrogram, and sometimes display fractionation or double or multiple components separated by very low-amplitude signals or an isoelectric interval.[3,4]

VT was induced by programmed stimulation after substrate mapping. An activation map was created if the VT was sustained and hemodynamically stable. Radiofrequency energy was delivered targeting the VT isthmus with an open-irrigated ablation catheter (IntellaNav or IntellaTip MiFi OI, Boston Scientific). After VT termination, additional ablation was performed targeting areas with LAVAs. If the VT was hemodynamically poorly tolerated, ablation was performed based on LAVA and pace mapping. Power settings of 30 to 50 W in the endocardium and 25 to 35 W in the epicardium were used. Procedural endpoints were VT isthmus ablation, LAVA elimination, and VT non-inducibility.

Lumipoint algorithm and offline analysis

Maps were analyzed retrospectively using a Rhythmia research review station (Boston Scientific). The confidence mask threshold was set to 0.020 mV, and signals above this threshold were annotated for the substrate map. The locations and areas of scar, which was defined by a local voltage of <1.5 mV, were assessed on the voltage map (Fig. 1A). The size of the scar was measured manually. The Lumipoint algorithm was then applied.

The "activation search" feature (Fig. 1B) was used to highlight areas with LPs. This tool allows one to select a portion of the mapping window, within which the software highlights activated regions during a given period. The search window was adjusted to cover the post-QRS period to identify areas with LPs. The "complex activation" feature (Fig. 1C) was used to highlight areas with FPs. This algorithm highlights regions of the map that exhibit multiple activation components within the search window. The minimum number of components was set to 7. The search window was adjusted to examine the entire mapping window. The "split activation" feature (Fig. 1D) was used to highlight areas with DPs. This algorithm highlights regions of the map with split potentials separated by at least 10 ms.

The accuracy of the automatic annotation system was evaluated by (1) assessing its correlation with manual annotation performed during the procedure, and (2) re-evaluating local electrograms within automatically annotated areas. The influence of the cardiac rhythm during mapping and the location of scar was also examined.

Automatically annotated areas were defined as those with LP, FP, or DP as per the Lumipoint algorithms. Manually annotated areas were defined as ablation sites and areas with LAVAs as determined manually during the procedure. Manually annotated areas were measured by tracing the areas with manually tagged points. The correlation between the automatically and manually annotated areas were assessed by measuring the overlaps between them. To limit subjectivity in these measurements,, two observers (Y.N and F.S) independently evaluated the correlation. If the results differed among the observers, the conclusion was decided through discussion. Automatically annotated areas were considered to match manually annotated areas when their respective areas overlapped by ≥90%. Automatic annotation was regarded as better if the automatically annotated area exceeded the manually annotated

area by equal or more than 10%, and the manual annotation was better if the opposite was observed.

Local potentials of all areas with LP, FP, or DP were re-evaluated and LAVAs confirmed manually as described above.[3,4] The percent area of these automatically annotated areas with manually confirmed LAVAs was calculated (termed "percent with LAVA" or %LAVA). %LAVA was examined and compared based on cardiac rhythm during mapping and location of scar.

Statistical analysis

Continuous variables are presented as mean ± standard deviation. Between-group comparisons were performed using unpaired Student's *t*-tests for continuous variables and χ^2 tests for categorical variables. Comparisons between multiple groups were performed using one-way analysis of variance (ANOVA) followed by Bonferroni-adjusted pairwise comparisons when significant. A P value of <0.05 (two-tailed) was accepted as statistically significant for all tests. Statistical analyses were performed using SPSS statistical software for Windows version 16.0 (SPSS Inc., Chicago, IL).

RESULTS

Patient characteristics

Baseline patients characteristics are summarized in Table 1. The mean patient age was 62 ± 14 years and the mean left ventricular ejection fraction was 39 ± 13%. Seventy-five patients (75%) had ischemic heart disease, and 25 patients (25%) had non-ischemic heart diseases (9 with dilated cardiomyopathy, 2 with hypertrophic cardiomyopathy, 6 with arrhythmogenic right ventricular cardiomyopathy, 3 with congenital heart disease, 2 with valvular heart disease, 2 with prior myocarditis, and 1 patient with cardiac sarcoidosis).

Electroanatomical mapping data

Electroanatomical mapping data are summarized in Table 2. Endocardial LV, endocardial RV, and epicardial maps were created in 83 (83%), 8 (8%), and 9 patients (9%), respectively. On average, 9976 ±

7477 points were acquired per map over 31 ± 11 minutes with a greater number in the epicardium than in other chambers (epicardium, 24500 ± 16160; LV, 8328 ± 3722; RV, 10700 ± 4990; $P < 0.001$ for epicardium vs. LV or RV). The total scar area was 80 ± 52 cm^2 and was larger in the LV than in RV (87 ± 54 cm^2 vs. 37 ± 20 cm^2; $P = 0.026$). The manually annotated area amounted to 35 ± 18 cm^2 and was larger in the LV than in the RV (36 ± 19 cm^2 vs. 18 ± 10 cm^2; $P = 0.025$). Areas with LP, FP, and DP as identified using automatic annotation were 19 ± 15 cm^2, 21 ± 16 cm^2, and 22 ± 16 cm^2, respectively. LP and DP areas were similar between mapped chambers; however, the FP area was larger in the LV than in RV (22 ± 16 cm^2 vs. 7 ± 5 cm^2; $P = 0.027$). The overlap among areas with LP, FP, and DP was 25 ± 22 cm^2. Consequently, the total automatically annotated area amounted to 38 ± 19 cm^2 and was not different between mapped chambers.

Correlation between automatic and manual annotation

During sinus rhythm, areas with LP, FP, and DP covered $37 \pm 25\%$, $45 \pm 33\%$, and $30 \pm 23\%$ of manually annotated areas, respectively. During RV pacing, the corresponding values were $24 \pm 22\%$, $45 \pm 25\%$, and $29 \pm 19\%$: and during LV pacing were $18 \pm 30\%$, $34 \pm 37\%$, and $15 \pm 15\%$. These areas complemented one other and collectively covered manually annotated areas (Fig. 1). The correlation between areas identified by automatic and manual annotation are summarized in Table 3. Overall, automatically annotated areas matched manual annotation in 64 patients (64%) and automatic annotation identified areas of LAVAs that were missed during manual annotation (automatic annotation better) in 15 patients (15%), with 3 cases (3%) in which this difference exceeded 30%. However, automatic annotation missed areas that were identified during manual annotation in 18 patients (18%), with this exceeding 30% in 3 cases (3%). In the 3 remaining patients, no clear substrate was identified during mapping and VT exhibited a centrifugal pattern, suggesting a non-reentrant VT mechanism. Ablation was performed in area with normal potentials. Therefore, comparison between manual and automatic annotation could not be performed.

Nearly all areas that were identified through automatic annotation but missed during manual annotation exhibited LAVAs of exceptionally low voltage (Fig. 2). In contrast, manual annotated areas that were missed by automatic annotation exhibited fragmented or split electrogram but with few activation components and short intervals between the components, therefore not entering in the definition of the algorithm.

When stratified by chamber mapped, automatic annotation was as accurate or more accurate at detecting LAVAs than manual annotation in 83% of patients in the LV (annotation match in 69% and automatic annotation better in 14%). However, automatic annotation was less accurate in the RV and epicardium; automatic annotation was as accurate or more accurate at detecting LAVAs than manual annotation in 63% of patients in the RV (annotation match in 50% and automatic annotation better in 13%) and in 66% in the epicardium (annotation match in 33% and automatic annotation better in 33%).

Impact of the cardiac rhythm and scar location on the accuracy of automatic annotation

%LAVA in areas with LP, FP, and DP were $56 \pm 32\%$, $86 \pm 14\%$, and $56 \pm 23\%$, respectively. %LAVA as a function of cardiac rhythm during mapping and scar location are described in Table 4. Substrate mapping was performed during sinus rhythm, RV pacing, and LV pacing in 34, 63, and 3 patients, respectively. The cardiac rhythm during mapping did not affect %LAVA in the areas with FP (sinus rhythm $86 \pm 18\%$, RV pacing $87 \pm 11\%$, LV pacing $79 \pm 6\%$, $P = 0.544$) or areas with DP (sinus rhythm $50 \pm 23\%$, RV pacing $60 \pm 22\%$, LV pacing $53 \pm 9\%$, $P = 0.095$). However, %LAVA was significantly higher during sinus rhythm than during RV pacing in areas with LP ($72 \pm 25\%$ vs. $47 \pm 33\%$, $P = 0.001$).

During sinus rhythm, %LAVA in areas with LP or FP were relatively high regardless of scar location, whereas %LAVA in areas with DP differed based on scar location ($P = 0.037$). Specifically, %LAVA in areas with DP were low in patients with RV scar ($22 \pm 20\%$) and epicardial scar ($37 \pm 15\%$). During RV pacing, %LAVA in areas with FP were high regardless of scar location, whereas those in areas with LP or DP were affected by scar location (LP area, $p = 0.001$; DP area, $p = 0.048$). %LAVA in areas with LP were large in patients with LV lateral wall scar ($76 \pm 19\%$) and small in patients with LV septal

scar ($37 \pm 27\%$), LV apical scar ($35 \pm 30\%$), and epicardial scar ($25 \pm 39\%$). %LAVA in areas with DP were low in patients with RV scar ($46 \pm 21\%$) and epicardial scar ($34 \pm 13\%$). We could not assess the impact of the scar location on %LAVA during LV pacing because of a small number of cases.

Notably, some DP areas were inappropriately annotated because of artifacts, especially in the RV apex and epicardium.

DISCUSSION

We found that the three automatic annotation features complemented each other and collectively identified manually annotated areas. Automatic annotation had equal or better accuracy than manual annotation in 79% of patients (annotation match in 64% and automatic annotation better in 15%), and the automatic annotation performed best in the LV relative to the RV or epicardium. Automatic FP annotation accurately detected LAVAs irrespective of cardiac rhythm during mapping and scar location; automatic LP annotation accurately detected LAVAs during sinus rhythm, but its performance was affected by scar location during RV pacing as activation of LV lateral wall is always delayed in this situation. The accuracy of automatic DP annotation was suboptimal in cases of RV or epicardial scar.

Discrepancies between automatic and manual annotations

Certain discrepancies were observed between areas identified by automatic versus manual annotation. Automatically annotated areas that were missed by manual annotation usually demonstrated very low voltage potentials, suggesting that these signals are more easily missed during procedures relying solely on manual annotation as the operator must distinguish LAVAs from artifacts in real-time. Manually annotated areas that were not identified using automatic annotation exhibited LAVAs that did not meet the algorithm's criteria for automatic annotation. Further investigation to determine whether and to what extent this can be minimized by optimizing settings of the algorithm for LAVA detection are warranted.

Factors affecting the accuracy of automatic annotation

Automatic LP annotation is performed by adjusting the search window to the post-QRS phase. Thus, its ability to detect delayed potentials requires that local activation be temporally distinct from the QRS complex. However, even in cases of conduction delays,[16] local activation can end within the QRS complex, leading to the inability of recognizing these potentials by the automatic LP annotation. This might be due to a proximity of the area of interest to the origin of ventricular activation. For example, during RV pacing, the earliest LV activation occurs at the interventricular septum, followed by lateral LV wall activation at the end. Thus, although septal activation is delayed, it is early relative to the window of interest and would therefore not automatically be recognized as a LP (Fig. 3). In contrast, the delay in local activation at the LV lateral wall would be sufficient to be correctly detected. Accordingly, the sensitivity of automatic LP annotation was high during RV pacing in patients with scar in the lateral LV but the specificity of LP detection in the lateral LV wall was decreased. During sinus rhythm, assuming a normal conduction system, electrical activation rapidly propagates through both ventricles, resulting in their simultaneous activation. In this situation, automatic LP annotation can identify delayed potentials correctly.

Automatic DP annotation frequently highlighted areas with artifacts. Reasons for the relatively low accuracy of automatic DP annotation in the RV and epicardium are unclear, but may be due to implantable cardioverter-defibrillator leads (often placed at the RV apex) and a heightened effect of breathing or body movements while mapping in the enclosed epicardial space, rendering electrograms from both of these chambers more susceptible to artifacts.

In contrast, automatic FP annotation exhibited higher accuracy and was not affected by pacing site or scar location. Since FP annotation recognizes multiple components of the electrogram, it may be less easily misled by artifacts. Furthermore, with FP annotation, local conduction delays were appropriately detected as the fragmentation of the local potential is independent of its timing relative to the QRS complex.

Clinical implications

13

The high correlation between automatic and manual annotation in our study allow to reliably replace manual annotation. Therefore, the procedure time could be shortened by using an automatic system for LAVA detection. Moreover, automatic annotation may improve the detection of low-voltage LAVAs, which are often missed during the procedure. However, although the sensitivity of this automatic annotation system for LAVA is relatively high, its specificity is less consistent. Therefore, at present, its algorithms are probably best used to suggest areas of interest that should then be confirmed manually.

Our results suggest that FP annotation could be the most useful for detecting LAVAs because it was less influenced by rhythm or scar location. However, LP and DP annotations serve to complement FP annotation, therefore they should not be dismissed when seeking to identify LAVAs.

In general, we should use the map created during sinus rhythm for LP annotation because mapping during sinus rhythm instead of RV pacing may improve LP annotation accuracy. However, if the scar location is known preoperatively, adapting the pacing site based on scar location could yield important insights on the VT substrate. For instance, RV pacing may be optimal for detecting LP near scar located on the LV lateral wall, whereas LV pacing may be useful for detecting LP near LV septal or RV scar (Fig. 4). Moreover, we should avoid using DP annotation in the RV and epicardium, where frequent artifacts may reduce the accuracy of the DP annotation.

Study limitations

Our study has several limitations. First, since the relationship between automatic and manual annotation was compared retrospectively, it remains unclear whether automatic annotation can improve the efficiency or outcomes of VT ablation. Prospective studies that use automatic annotation in real-time would best address this question. Second, the complex distribution of automatically annotated areas prevented us from analyzing the overlap among different automatic annotation features. Finally, manual annotation was performed by operators during the procedure and may have a subjective component. However, all ablation procedures were performed by experienced operators in this study.

CONCLUSION

In patients with scar-related VT, automatically annotating LAVAs with the Lumipoint algorithm showed good correlation with manual annotation. Although the accuracies of automatic annotation features are affected by the patient's rhythm and the location of scar, their combined use can appropriately identify areas with LAVAs.

REFERENCES

1. Santangeli P, Frankel DS, Tung R, Vaseghi M, Sauer WH, Tzou WS, Mathuria N, Nakahara S, Dickfeldt TM, Lakkireddy D, Bunch TJ, Di Biase L, Natale A, Tholakanahalli V, Tedrow UB, Kumar S, Stevenson WG, Della Bella P, Shivkumar K, Marchlinski FE, Callans DJ; International VT Ablation Center Collaborative Group. Early mortality after catheter ablation of ventricular tachycardia in patients with structural heart disease. J Am Coll Cardiol 2017;69:2105-2115.

2. Tung R, Vaseghi M, Frankel DS, Vergara P, Di Biase L, Nagashima K, Yu R, Vangala S, Tseng CH, Choi EK, Khurshid S, Patel M, Mathuria N, Nakahara S, Tzou WS, Sauer WH, Vakil K, Tedrow U, Burkhardt JD, Tholakanahalli VN, Saliaris A, Dickfeld T, Weiss JP, Bunch TJ, Reddy M, Kanmanthareddy A, Callans DJ, Lakkireddy D, Natale A, Marchlinski F, Stevenson WG, Della Bella P, Shivkumar K. Freedom from recurrent ventricular tachycardia after catheter ablation is associated with improved survival in patients with structural heart disease: An International VT Ablation Center Collaborative Group study. Heart Rhythm 2015;12:1997-2007.

3. Jaïs P, Maury P, Khairy P, Sacher F, Nault I, Komatsu Y, Hocini M, Forclaz A, Jadidi AS, Weerasooryia R, Shah A, Derval N, Cochet H, Knecht S, Miyazaki S, Linton N, Rivard L, Wright M, Wilton SB, Scherr D, Pascale P, Roten L, Pederson M, Bordachar P, Laurent F, Kim SJ, Ritter P, Clementy J, Haïssaguerre M. Elimination of local abnormal ventricular activities: a new end point for substrate modification in patients with scar-related ventricular tachycardia. Circulation 2012;125:2184-2196.

4. Sacher F, Lim HS, Derval N, Denis A, Berte B, Yamashita S, Hocini M, Haissaguerre M, Jaïs P.

Substrate mapping and ablation for ventricular tachycardia: the LAVA approach. J Cardiovasc Electrophysiol 2015;26:464-471.

5. Santangeli P, Marchlinski FE. Substrate mapping for unstable ventricular tachycardia. Heart Rhythm 2016;13:569-583.

6. Cassidy DM, Vassallo JA, Buxton AE, Doherty JU, Marchlinski FE, Josephson ME. The value of catheter mapping during sinus rhythm to localize site of origin of ventricular tachycardia. Circulation 1984;69:1103−1110.

7. Soejima K, Suzuki M, Maisel WH, Brunckhorst CB, Delacretaz E, Blier L, Tung S, Khan H, Stevenson WG. Catheter ablation in patients with multiple and unstable ventricular tachycardias after myocardial infarction: short ablation lines guided by reentry circuit isthmuses and sinus rhythm mapping. Circulation 2001; 104:664-669.

8. Anter E, Tschabrunn CM, Buxton AE, Josephson ME. High-resolution mapping of postinfarction reentrant ventricular tachycardia: electrophysiological characterization of the circuit. Circulation 2016;134:314-327.

9. Martin R, Hocini M, Haïsaguerre M, Jaïs P, Sacher F. Ventricular tachycardia isthmus characteristics: insights from high-density mapping. Arrhythm Electrophysiol Rev 2019;8:54-59.

10. Martin CA, Takigawa M, Martin R, Maury P, Meyer C, Wong T, Shi R, Gajendragadkar P, Frontera A, Cheniti G, Thompson N, Kitamura T, Vlachos K, Wolf M, Bourier F, Lam A, Duchâteau J, Massoullié G, Pambrun T, Denis A, Derval N, Hocini M, Haïssaguerre M, Jaïs P, Sacher F. Use of novel electrogram "Lumipoint" algorithm to detect critical isthmus and abnormal potentials for ablation in ventricular tachycardia. JACC Clin Electrophysiol 2019;5:470-479.

11. Frontera A, Melillo F, Baldetti L, Radinovic A, Bisceglia C, D'Angelo G, Foppoli L, Gigli L, Peretto G, Cireddu M, Sala S, Mazzone P, Della Bella P. High-density characterization of the ventricular electrical substrate during sinus rhythm in post-myocardial infarction patients. JACC Clin Electrophysiol 2020;6:799-811.

12. Takigawa M, Martin CA, Derval N, Denis A, Vlachos K, Kitamura T, Frontera A, Martin R, Cheniti

G, Lam A, Bourier F, Thompson N, Wolf M, Massoulié G, Escande W, Andre C, Zeng LJ, Nakatani Y, Roux JR, Duchateau J, Pambrun T, Sacher F, Cochet H, Hocini M, Haissaguerre M, Jais P. Insights from atrial surface activation throughout atrial tachycardia cycle length: A new mapping tool. Heart Rhythm 2019;16:1652-1660.

13. Alken FA, Klatt N, Muenkler P, Scherschel K, Jungen C, Akbulak RO, Kahle AK, Gunawardene M, Jularic M, Dinshaw L, Hartmann J, Eickholt C, Willems S, Stute F, Mueller G, Blankenberg S, Rickers C, Sinning C, Zengin-Sahm E, Meyer C. Advanced mapping strategies for ablation therapy in adults with congenital heart disease. Cardiovasc Diagn Ther 2019;9:S247-S263.

14. Solimene F, Maddaluno F, Malacrida M, Schillaci V. Pseudo-reentry due to automatic annotation of dissociated activity unmasked by the new Lumipoint™ algorithm. Clin Case Rep 2019;8:38-40.

15. Bisceglia C, Frontera A, Della Bella P. The LUMIPOINT™ software: are we just at the turning point? Europace 2019;21:iii25-iii26.

16. de Bakker JM, van Capelle FJ, Janse MJ, Tasseron S, Vermeulen JT, de Jonge N, Lahpor JR. Slow conduction in the infarcted human heart. 'Zigzag' course of activation. Circulation 1993;88:915-926.

TABLES

Table 1. Patient characteristics

	n = 100

Age, years	62 ± 14
Sex, male	87 (87)
Left ventricular ejection fraction, %	39 ± 13
Etiology of heart disease	
Ischemic	75 (75)
Non-ischemic	25 (25)
Implantable cardioverter-defibrillator	73 (73)
Cardioversion or defibrillation prior to ablation	43 (43)
Arrhythmic storm prior to ablation	26 (26)

Data are presented as mean ± SD or number (%) of patients.

Table 2. Electroanatomical mapping data

	Total (n = 100)	LV (n = 83)	RV (n = 8)	Epicardium (n = 9)	P value

Mapping points	9976 ± 7477	8328 ± 3722	10700 ± 4990	24500 ± 16160[†]	< 0.001
Mapping duration, mins	31 ± 11	30 ± 10	34 ± 14	38 ± 7	0.076
Scar area, cm^2	80 ± 52	87 ± 54[*]	37 ± 20	56 ± 28	0.011
Manually annotated area, cm^2	35 ± 18	36 ± 19	18 ± 10	38 ± 14	0.026
Automatically annotated area, cm^2	38 ± 19	38 ± 19	27 ± 14	43 ± 19	0.200
LP area, cm^2	19 ± 15	18 ± 14	19 ± 18	27 ± 15	0.189
FP area, cm^2	21 ± 16	22 ± 16[*]	7 ± 5	24 ± 20	0.029
DP area, cm^2	22 ± 16	22 ± 17	14 ± 9	27 ± 13	0.197
Overlap among LP, FP, and DP areas, cm^2	25 ± 22	25 ± 22	13 ± 9	35 ± 27	0.106

Data are presented as mean ± SD or number (%) of patients. [*]P < 0.050 vs. RV. [†]P < 0.001 vs. LV and RV.

DP, double potential; FP, fragmented potential; LP, late potential; LV, left ventricle; RV, right ventricle.

Table 3. Correlation between automatically and manually annotated areas

	Total (n = 100)	Left ventricle (n = 83)	Right ventricle (n = 8)	Epicardium (n = 9)
Identical	64 (64)	57 (69)	4 (50)	3 (33)

	Total	LV septum	LV anterior	LV lateral
Automatic annotation better				
10-30%	12 (12)	8 (10)	1 (13)	3 (33)
> 30%	3 (3)	3 (4)	0 (0)	0 (0)
Manual annotation better				
10-30%	15 (15)	12 (14)	2 (25)	1 (11)
> 30%	3 (3)	1 (1)	0 (0)	2 (22)
No comparison	3 (3)	2 (2)	1 (13)	0 (0)

Data are presented as number (%) of patients.

Table 4. Accuracy of automatically annotated areas regarding the scar location and mapping rhythm.

	Total	LV septum	LV anterior	LV lateral	LV inferior	LV apex	RV	Epicardium	P value

	(n = 100)	(n = 30)	(n = 31)	(n = 23)	(n = 34)	(n = 11)	(n = 7)	(n = 8)	
Sinus rhythm, n	34	7	12	4	11	6	4	3	
%LAVA in LP area, %	72 ± 25	72 ± 34	75 ± 32	91 ± 11	74 ± 23	83 ± 22	65 ± 12	78 ± 5	0.822
%LAVA in FP area, %	86 ± 18	88 ± 25	89 ± 23	93 ± 9	87 ± 11	90 ± 13	82 ± 13	82 ± 11	0.975
%LAVA in DP area, %	50 ± 23	62 ± 24	65 ± 19	61 ± 23	53 ± 18	54 ± 29	22 ± 20*	37 ± 15	0.037
RV pacing, n	63	22	18	19	23	4	3	5	
%LAVA in LP area, %	47 ± 33	37 ± 27	51 ± 28	76 ± 19†	51 ± 33	35 ± 30	48 ± 33	25 ± 39	0.001
%LAVA in FP area, %	87 ± 11	89 ± 12	90 ± 10	89 ± 12	84 ± 12	83 ± 8	82 ± 16	81 ± 8	0.423
%LAVA in DP area, %	60 ± 22	64 ± 22	68 ± 21	66 ± 23	61 ± 16	54 ± 32	46 ± 21	34 ± 13*	0.048
LV pacing, n	3	1	1	0	1	1	0	0	
%LAVA in LP area, %	56 ± 29	84	26	NA	59	26	NA	NA	NA
%LAVA in FP area, %	79 ± 6	73	79	NA	84	79	NA	NA	NA
%LAVA in DP area, %	53 ± 9	60	57	NA	43	57	NA	NA	NA

Data are mean ± SD. When a case has scars in multiple segments, the case is included in the multiple groups of the scar location. *$P < 0.010$ and †$P < 0.001$ vs. other scar locations. DP, double potential; FP, fragmented potential; LP, late potential; LV, left ventricle; RV, right ventricle; %LAVA, percent with local abnormal ventricular activity.

FIGURES
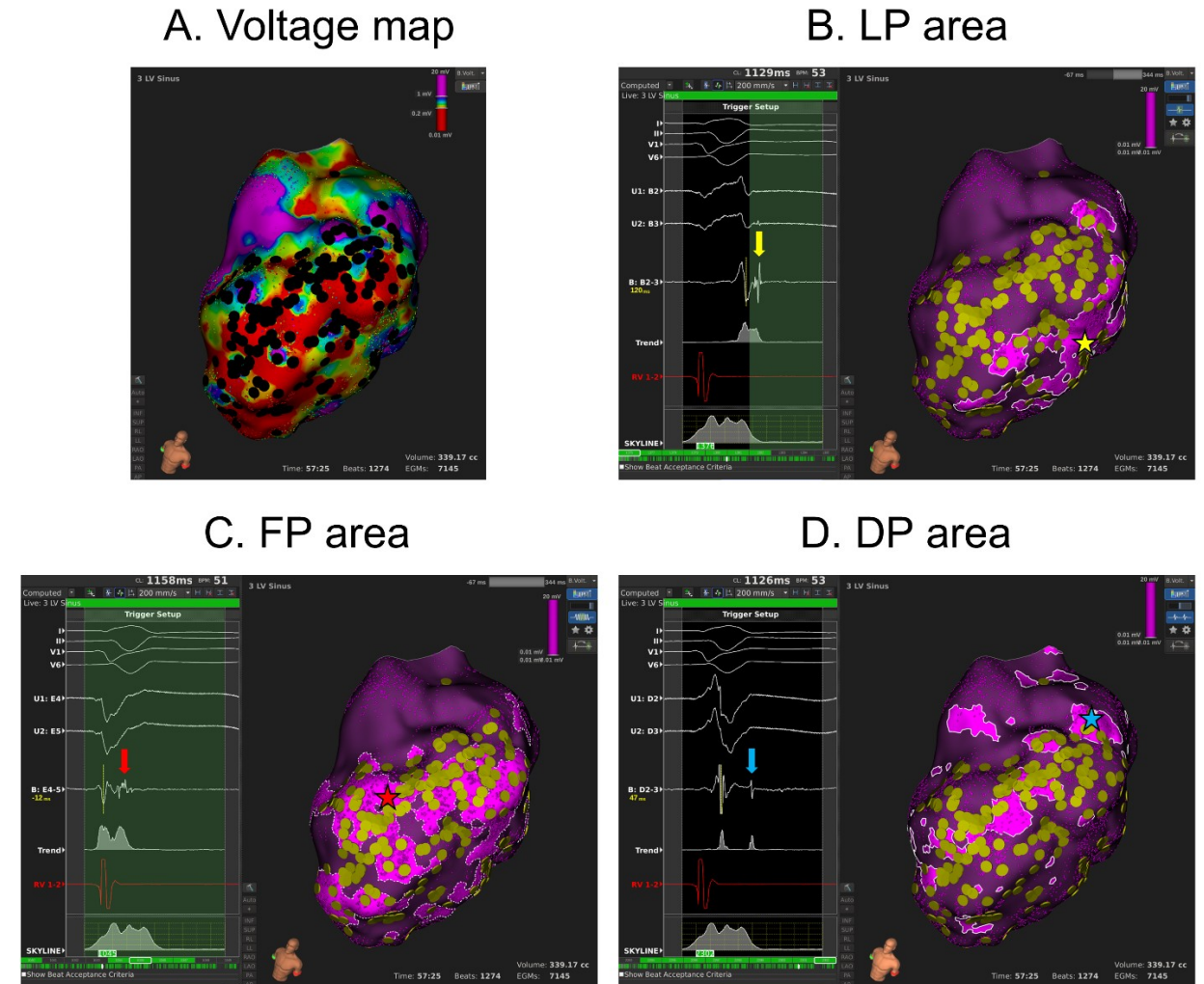
Figure 1. Representative correlation between automatically and manually annotated areas.
Tags on the maps indicate manually annotated areas. (A) Manually annotated areas were distributed throughout the area of scar in the voltage map. (B) The "activation search" feature was used to annotate late potential (LPs). The search window (green curtain) was adjusted to analyze the post-QRS phase. A representative LP (yellow arrow) is shown within the highlighted area (yellow star). (C) The "complex activation" feature was used to annotate fragmented potentials (FPs). The search window was adjusted to cover the full mapping window. A representative multi-component potential (red arrow) is shown within the highlighted area (red star). (D) The "split activation" feature was used to annotate double potentials (DPs). A

representative split potential (blue arrow) is shown within the highlighted area (blue star). Different algorithms supplemented missing parts in each feature, and the automatically annotated area completely covered the manually annotated area.

A. Voltage map

B. FP area during RV pacing
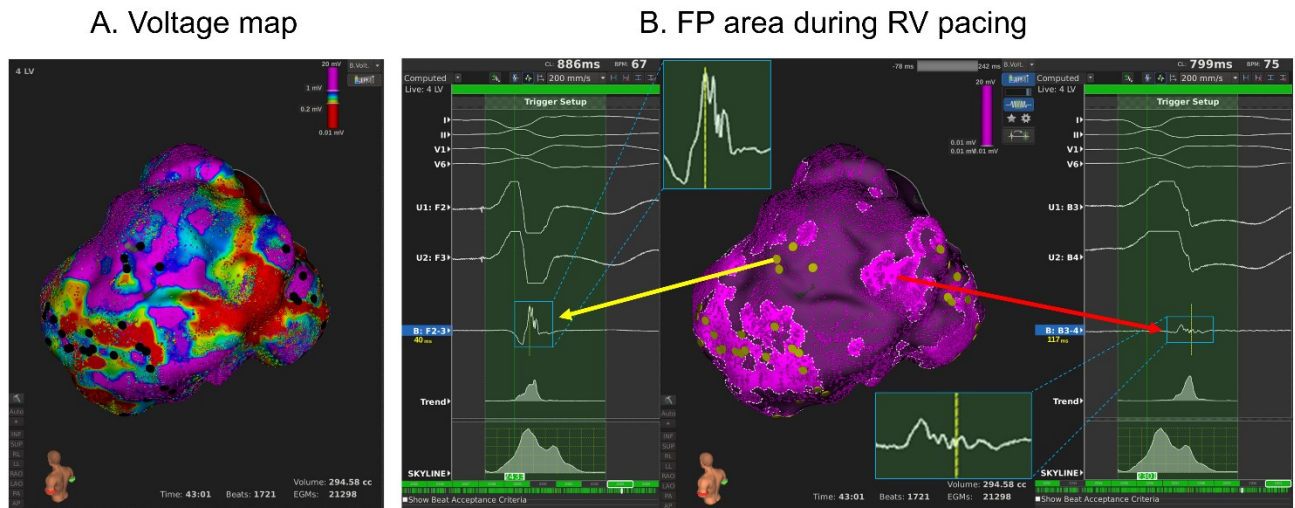
Figure 2. The mechanisms of discrepancies between automatically and manually annotated areas. Tags on the map correspond to manually annotated areas with local abnormal ventricular activities (LAVAs). (A) In the voltage map, a scar area was identified on the left ventricular (LV) lateral wall. (B) The "complex activation" feature was applied to identify fragmented potentials (FPs). An area that was identified through automatic annotation but missed during manual annotation exhibited a low-voltage LAVA (red arrow). In contrast, a manually annotated area that was missed by automatic annotation exhibited fragmented electrogram but with few activation components and short intervals between the components.

A. Voltage map   B. LP area during RV pacing
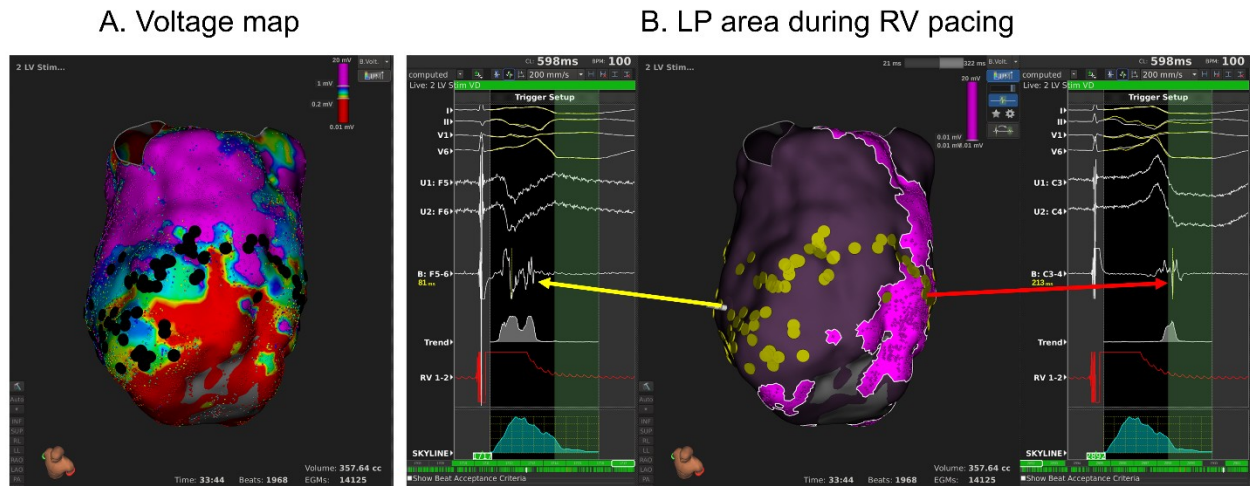
Figure 3. The impact of scar location on automatic late potential (LP) annotation.
Tags on the map correspond to manually annotated areas. (A) In the voltage map, an area of scar was identified extending from the septum to lateral wall of the left ventricle (LV). (B) The "activation search" feature with the search window (green curtain) on the post-QRS phase was applied. The long-duration potential in the lateral wall was correctly annotated (red arrow). However, that in the LV septum (yellow arrow) was not detected by the automatic LP annotation since this potential ended before the end of the QRS complex but it was detected by the FP algorithm. Another interesting point in this figure is the extent of post QRS potentials area (highlighted area on panel B) that extents much more than the true LAVA area due to the delayed activation on the lateral LV wall during RV pacing.

A. Voltage map   B. LP area during RV pacing   C. LP area during LV pacing
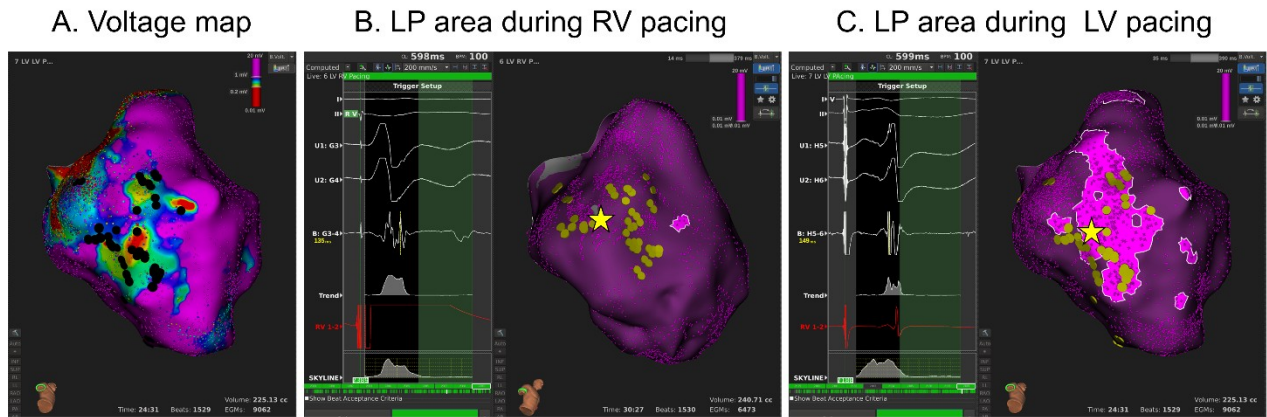
Figure 4. Comparison of automatic late potential (LP) annotation during right versus left ventricular pacing.

Tags on the map show manually annotated areas. The "activation search" feature was used to annotate late potentials (LPs). The search window (green curtain) was adjusted to cover the post-QRS phase. (A) The voltage map shows a left ventricular (LV) septal scar, and abnormal potentials distributed around the scar. (B) During right ventricular (RV) pacing, automatic LP annotation did not highlight the area of local abnormal ventricular activity (LAVA) on the LV septum (yellow star) because of its relatively early onset. (C) During LV pacing, however, the LAVA on the LV septum was correctly detected because its onset was relatively delayed.